A facile route to self-assembled Hg//MoSI nanowire networks†

Valeria Nicolosi,*[a] Zabeada Aslam,[a] Kasim Sader,[bc] Gareth M. Hughes,[a] Damjan Vengust,[de] Neil P. Young,[a] Ron Doole,[a] Dragan Mihailovic,[de] Andrew L. Bleloch,[bc] Angus I. Kirkland,[a] Nicole Grobert[a] and Peter D. Nellist[a]

Received (in Montpellier, France) 31st March 2010, Accepted 4th May 2010
DOI: 10.1039/c0nj00237b

Nanotechnology crucially depends on new molecular-scale materials with tunable properties. In molecular electronics, building blocks have been reduced to single molecules, while connectors have largely remained at the mesoscopic scale. As a result, the behaviour of such devices is largely governed by interface effects and hence, currently, attention is focused on finding suitable molecular-scale alternatives. In this paper we discuss a new generation of one-dimensional inorganic nanostructures aimed at to replacing the mesoscopic connectors currently used in the electronics industry. We demonstrate how chemical functionalisation of nanowires consisting of molybdenum, sulphur and iodine in conjunction with very low concentrations of molecular mercury leads to one-dimensional systems which can be easily connected opening up new pathways to controlled deposition and interface formation.

1. Introduction

One-dimensional nanotubes and nanowires show potential for playing an important role in future nanotechnological applications, e.g. in areas ranging from molecular-scale logic elements[1] to advanced sensors.[2] However, there are many hurdles that need to be overcome in order to efficiently progress in this area of research. For example, the efficiency of such molecular devices strongly depends on the quality of the contacts between individual building blocks, on the ability to self-assemble following well controlled routes, allowing the formation of large circuits and more importantly on their recognitive ability to connect to diverse materials (*i.e.* gold metal surfaces for connections to outside world; biomolecules for nano-sensors, nano-electrodes and molecular switches). Long thought to be ideal candidates for the scope due to their remarkable electrical and mechanical properties,[3] carbon nanotubes (CNTs) ultimately have shown to have limited application in this field. Along with a lack of electronic uniformity, difficult liquid-phase processing in low-boiling point media[4] and challenging spontaneous structuring into larger circuits (mainly due to the fact that CNTs are usually very entangled and exist in a broad range of diameters going between 0.6 and 2 nm) have proven to be the main limiting factors for carbon nanotubes.

Although, connectivity at the CNTs ends was achieved via attaching linking groups, however, these are typically not conducting, greatly limiting their suitability as molecular interconnects. In this context, the family of molecular nanowires made of molybdenum, sulphur and iodine ($Mo_6S_{9-x}I_x$)[5] have attracted much attention in the last few years being considered as highly suitable building blocks for molecular electronic devices. These nanowires possess similar mechanical and electrical properties as CNTs[6–10] with the great advantage of having uniform electrical behaviour, showing linear *I–V* characteristics and metallic behaviour in the Ohmic regime.[11,12] The ability of these MoSI materials to completely de-bundle into isolated, 0.96 nm wide nanowires (their diameter is defined by their molecular structure and hence is uniform from nanowire to nanowire) by simple dispersion in common low-boiling point solvents[9,10] constitutes a major advantage. Previous studies[9] have shown de-bundling by dilution, *i.e.* solutions solely consisting of isolated wires and very small bundles of two or three nanowires at concentrations below 0.003 mg ml^{-1}, making these nanowires very easily processable by conventional wet-chemistry. Unlike other kinds of crystalline nanowires, these molecular nanowires are composed of repeating molecular units consisting of $Mo_6S_{9-x}I_x$ clusters, which are joined together by sulphur bridges,[13] that terminate the nanowires in the majority of the cases (Fig. SI1). The presence of sulphur and iodine within the structure makes these nanowires readily accessible to form chemical bonds with very diverse molecular entities ensuring good transport and contacting properties. The possibility of randomly connecting MoSI nanowires at their sulphur terminations through bridging gold nanoparticles has been successfully demonstrated.[14] However, for functional nanodevices it is necessary to control the

[a] *Department of Materials, University of Oxford, Parks Road, Oxford, UK OX1 3PH. E-mail: valeria.nicolosi@materials.ox.ac.uk; Tel: +44 (0)1865 273672, +44 (0)1865 283740*
[b] *SuperSTEM Laboratory, STFC Daresbury, Keckwick Lane, Warrington, UK WA4 4AD*
[c] *University of Liverpool, Department of Engineering, Liverpool, UK L69 3GH*
[d] *Jozef Stefan Institute, Jamova 39, 1000 Ljubljana, Slovenia*
[e] *Mo6 d.o.o., Teslova 30, 1000 Ljubljana, Slovenia*

† Electronic supplementary information (ESI) available: NW structure; Sedimentation study; HAADF STEM of a sample cooled-down at cryo-temperatures and allowed to warm up to room temperature again; patterned deposition FIB experiment. See DOI: 10.1039/c0nj00237b

assembly process of the individual building blocks, thus paving the way for a pre-determined recognition of molecular species at specific positions. Such controlled assembly can only be accomplished by means of uniform and efficient chemical functionalisation of the nanowires.

Here, we present an innovative approach for nanowire functionalisation which can be applied to processing at the larger scale in order to control the deposition and interface formation of conductive molecular networks.

2. Experimental details

$Mo_6S_3I_6$ NW material synthesised from the constituent elements was obtained from Mo6 d.o.o.[5] Hg//$Mo_6S_3I_6$ complexes in acetone or water were prepared at nanowire concentrations of 0.1 mg ml^{-1} and at Hg/MoSI ratio of 1 to 10. The correspondent mercury concentrations used for the production of these systems is approximately 100 times below the EU RoHS Directive (2002/95/EC). All dispersions were first sonicated for 15 minutes using a Hielscher UP100H ultrasonic tip (50 W, 30 kHz), then for 2 hours in an Ultrawave U50 ultrasonic bath (100 W, 42 kHz). For sedimentation measurements a Hg//$Mo_6S_3I_6$ dispersion was transferred to a 1 cm path length quartz cuvette, and the transmission of laser pulses (λ = 650 nm, pulse duration 10 ms) through the centre of the sample monitored over the course of two weeks. Atomic force microscopy (AFM) studies were carried on both as prepared and aged Hg//$Mo_6S_3I_6$ solutions using a Park Scientific Instruments Autoprobe CP microscope operated in tapping mode using a Mikromash NSC35/AlBS tip (silicon, tip radius 10 nm, k = 4.5 N m^{-1}, ω = 150 kHz). For this purpose, deposition on freshly cleaved mica was performed by simple drop casting in ambient conditions. For electron microscopy characterisation the Hg//$Mo_6S_3I_6$ solutions at different ageing times were deposited on 400 mesh holey carbon on copper grids. Aberration-corrected (scanning) transmission electron microscopy, (S)TEM, images were taken with the Oxford-JEOL JEM2200MCO FEGTEM/STEM, fitted with two CEOS Cs aberration correctors, operated at 200 kV. Further aberration-corrected STEM characterisation was performed using a VG HB501 100 kV instrument fitted with a Nion Cs corrector. A JEOL 3000F TEM equipped with an Oxford Instruments INCA detector operated at 300 kV was used for energy-dispersive x-ray spectroscopy (EDX) analysis. In order to verify crystallisation upon cooling of the mercury coating the Hg//MoSI TEM sample was cooled down to liquid nitrogen temperature ($\sim$ −196 °C) *in situ* in the aberration-corrected FEGTEM/STEM JEM2200MCO microscope, using a custom made Fischioni ultra-low drift TEM cryo holder. *In situ* room temperature electrical measurements were performed using a Nanofactory TEM/STM holder in order to confirm the maintained metallicity of the Hg//MoSI nanowire complexes. The sample was mounted onto a 0.25 mm Au wire by dipping the wire into the Hg//MoSI nanowire solution. Subsequently, the solvent was left to evaporate. A tungsten probe was mounted onto piezo-electric actuator that can be moved in x, y and z-direction in order to establish electrical contact between the tip and individual bundles.

3. Results and discussion

3.1. Chemical functionalisation

Our choice of functionalising agent is based on two main factors: high affinity towards sulphur and iodine, followed by high solubility in common solvents to guarantee easy processability without changing the intrinsic properties of the nanowires. For these reasons, an organic salt of mercury, Mercury(II) acetate ($Hg(OAc)_2$), was chosen. In most organic liquid media $Hg(OAc)_2$ will spontaneously dissociates releasing Hg^{2+} ions:

$$Hg(OAc)_2 \rightleftarrows Hg^{2+} + (OAc)^-_2 \quad (1)$$

Mercury(II) has a high affinity for sulphur ligands, therefore, in presence of the MoSI nanowires, formation of Hg//MoSI complexes is possible. Atomic force microscopy (AFM) studies revealed that the as-prepared Hg//MoSI solution contained thin nanowire bundles with an average diameter of *ca.* 6 ± 4 nm as shown in Fig. 1a. The nanowires immediately after preparation are sparsely distributed on the substrate not showing any successful interconnection and self-assembly. Upon comparing these results with previous measurements on chemically unmodified MoSI nanowires[9,10] no appreciable difference in terms of average bundle diameter was observed. This suggests that either the Hg-salt did not interact with the nanowires at all or that the interaction did not promote the hoped nanowire network self-assembly. However, it is reasonable to assume that time will be required for the Hg-salt to dissociate in solution and for the released single mercury ions to interact with the sulphur and iodine atoms of the wires afterwards.

Nonetheless, the interaction between the nanowires and the functionalising agent is not expected to occur immediately, therefore the samples were stored under unperturbed conditions at room temperature over a period of one month, monitoring the evolution of the system over time. The stability of these dispersions over time was investigated by performing sedimentation measurements (Fig. SI2) over the course of 30 days showing that no sedimentation had occurred. Fig. 1b shows a representative AFM micrograph of the system after two weeks from preparation, showing nanowires closely interconnected to form highly structured networks. The cross sections of two representative wires shown as insets in

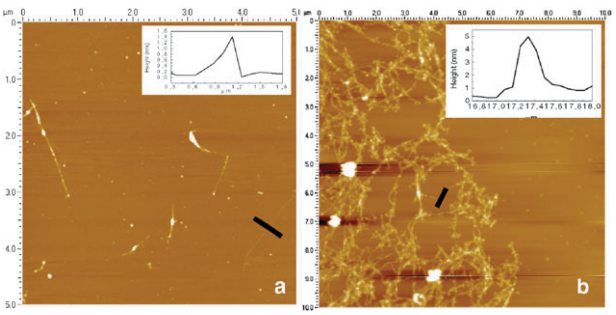

Fig. 1 Typical AFM images for Hg//MoSI Nanowire complexes immediately (a) and after two weeks (b) from preparation. Cross-sections of two representative nanowire bundles are presented as insets.

Fig. 1(a,b) reveal a 30% increase in the bundle diameter after allowing 2 weeks from the initial preparation. This observed change in diameter suggests a progression from free nanowires to Hg//MoSI nanowire complexes. Initially, the diameters appear smaller because the mercury is either only very loosely associated with the nanowires or not at all. Thus, to a first approximation, the diameter distributions at time zero from preparation represent the diameters of the nanowires alone, consistent with diameter data presented elsewhere for unfunctionalised nanowires dispersed in organic solvents only.[6,10] Over time the mercury ions appear to assemble on the side walls of the nanowires resulting in an increase in diameter as measured by AFM at longer times. However, AFM techniques are insufficient in order to identify whether the increase in nanowire diameter is due to the progressive accumulation of impurities. Transmission electron microscopy (TEM) and Energy Dispersive X-ray (EDX) spectroscopy were used to analyse the structural and chemical nature of these systems.

3.2. Electron microscopy studies—structure and morphology of Hg//$Mo_6S_3I_6$ complexes

A typical example of a multi-branched Hg//$Mo_6S_3I_6$ nanowire complex is shown in the TEM micrograph in Fig. 2a. The presence of mercury was confirmed in the EDX spectrum in Fig. 2b, acquired from the same wires as in Fig. 2a. The features of interest are the Mo Kα peak at 17.4 keV, the Mo Kβ at 19.6 keV, the joint Mo Lα and S Kα peaks at 2.3 keV, and the Hg Lα peak at 9.9 keV and Lβ at 11.9 keV. The secondary I Lα, Lβ1, Lβ2 and Lγ peaks do also appear at 3.9 keV, 4.22 keV, 4.5 keV and 4.8 keV respectively. The spectrum also shows an iron signal originating from the objective lens (Iron Kα and Kβ peaks at 6.4 keV and 7.06 keV respectively) and a copper contribution (Copper Kα at 8.046 eV and Kβ at 8.904 keV) from the TEM grid.

Previous aberration-corrected scanning transmission electron microscopy (STEM) studies showed that the $Mo_6S_3I_6$ nanowires are structurally terminated by sulphur trimers.[13] The high chemical affinity between sulphur and mercury explains why the free mercury ions in solution tend to interact preferentially with the sulphur atoms terminating the wires, hence playing a crucial role in the formation of the extended networks shown in Fig. 2a. Therefore, mercury interconnects vicinal wires end-to-end similarly to a soldering agent. In order to better understand the interaction established between the mercury and the nanowires, aberration-corrected high-resolution transmission electron microscopy (HRTEM) and high angle annular dark field scanning transmission electron microscopy (HAADF STEM) characterisation at different sample ageing times were performed, allowing us to observe the Hg//MoSI complex evolution in great detail. HAADF STEM is an exceptionally useful technique for studying these systems as it provides direct atomic probing, with image intensities dependent upon atomic number (Z-contrast).[15,16] Unlike HRTEM, which relies on coherence in order to generate phase-contrast images, HAADF gives rise to an incoherent imaging mode in which the detected signal scales directly with Z.[17] In these systems mercury possesses a much greater atomic number than any other atomic species present in the wires (Z_{Hg} = 80, Z_{Mo} = 42, Z_S = 16, Z_I = 53). Hence, Hg exhibits a much stronger scattering power, yielding higher intensities, correlating bright areas in the image with mercury rich regions. Fig. 3 shows representative images of the same Hg//MoSI sample recorded immediately after preparation (Fig. 3a,b) and after allowing to age for 4 weeks (Fig. 3c,d).

High-resolution HAADF micrographs taken immediately after sample-preparation (Fig. 3a,b), reveal the Hg being randomly clustered around the bundles, leaving large areas of the NWs uncoated. These images are similar to the HAADF images of unfunctionalised $Mo_6S_3I_6$ NWs dispersed in common organic solvents presented elsewhere.[13] One month after preparation the MoSI NW the walls appear to be completely coated with a thin layer of Hg (HAADF STEM in Fig. 3c and bright field STEM in Fig. 3d). Clearly, the diameter of the hybrid has increased significantly over time, supporting the AFM results shown earlier. This evidences the progressive formation of a Hg coating on the $Mo_6S_3I_6$ NWs. The Hg coating seems to adopt a completely disordered and amorphous form (Fig. 3c–d), with the NWs still preserving intact their typical crystalline structure underneath. One possible explanation for this is that the mercury ions initially

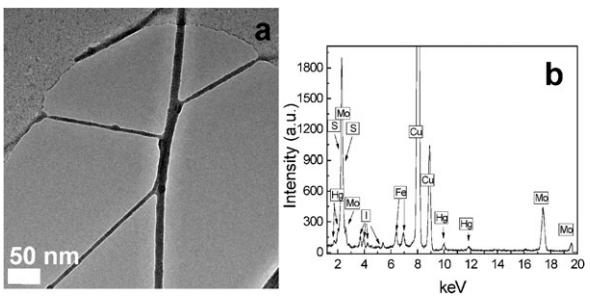

Fig. 2 (a) TEM image of a multi-branched Hg//$Mo_6S_3I_6$ nanowire complex; (b) Energy Dispersive X-ray (EDX) spectrum acquired from the same wires in (a).

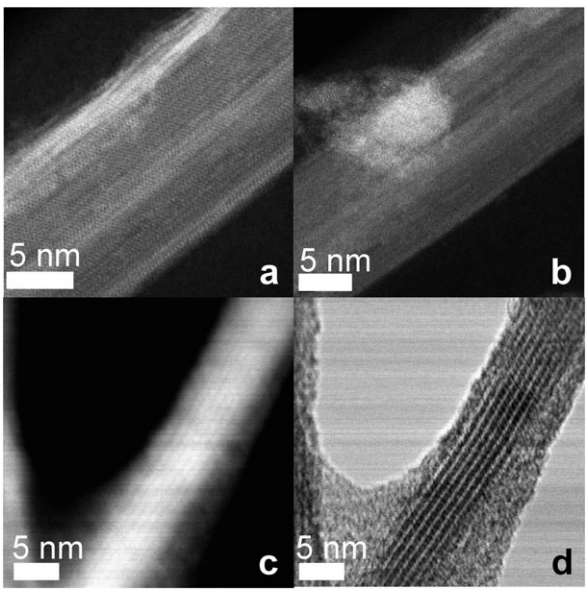

Fig. 3 HAADF STEM images of the Hg//MoSI complex immediately (a,b) and after four weeks (c,d) from preparation.

assemble on the side walls of the nanowires driven by their strong affinity with sulphur and iodine, which in this case function as nucleation sites. Over time further precipitation of mercury along the nanowires will occur due to the strong cohesive forces between the mercury atoms, resulting in a thin layer of liquid mercury around the nanowires. Assuming that mercury forms a liquid layer wetting the wires at room temperature, one would expect to observe a liquid–solid phase transition upon cooling of system below the mercury melting point (~ −38 °C). In order to verify this the Hg//MoSI sample of Fig. 3c,d was cooled down to liquid nitrogen temperature (~ −196 °C) *in situ* in an aberration-corrected FEGTEM/STEM microscope, using a custom made ultra-low drift TEM cryo holder. Crystallisation upon cooling was clearly shown by aberration-corrected HRTEM characterisation (Fig. 4).

Sub-nanometre mercury crystallites in the typical rhombohedral configuration (space group R-3 m, #166) are observed covering both the nanowire bundle surface (Fig. 4a) and the surrounding area of the supporting amorphous carbon of the TEM grid (Fig. 4b). Fig. 4b also shows both [100] and [110] projections of the mercury molecular crystal for comparison. This crystallisation process occurred upon cooling and the decoration of the $Mo_6S_3I_6$ nanowire surface with the mercury nanoclusters is even more evident from the aberration corrected HAADF images shown in Fig. 5, which illustrate representative

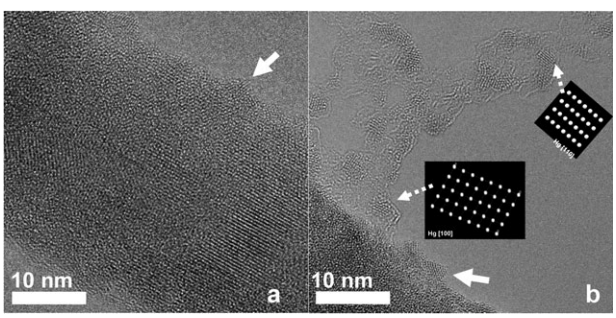

Fig. 4 *In situ* cryo-HRTEM of an aged sample showing crystallisation of the Hg upon cooling. Sub-nanometre Hg crystallites cover both the NW surface (a) and the surrounding area of the TEM grid (b). The [100] and [110] projections of the Hg molecular crystal are shown as insets in (b).

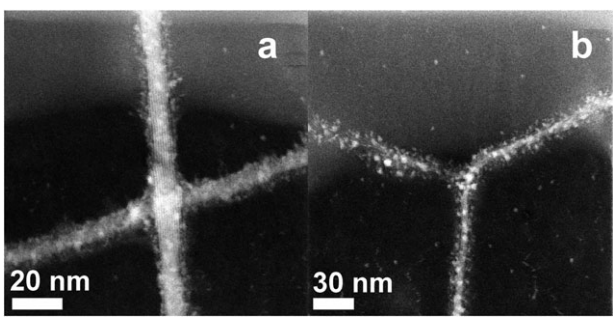

Fig. 5 *In situ* cryo-HAADF STEM images of an aged Hg//MoSI sample showing two very common architectures, a cross (a) and a Y-junction (b).

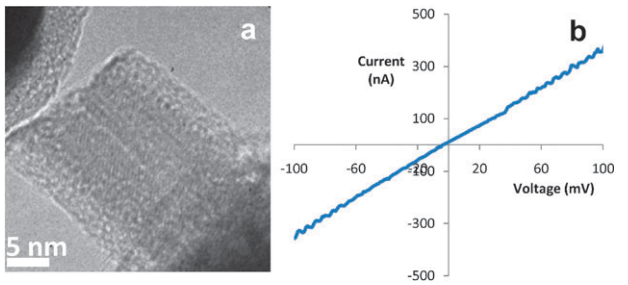

Fig. 6 (a) TEM image showing a small bundle of Hg//MoSI NWs mounted on a gold wire and in contact with a tungsten tip; (b) Current-voltage curve corresponding to the system in (a).

examples of two very common Hg//MoSI architectures, a cross (5a), a Y-junction (5b).

As a further test of the reversible nature of the phase transition involved, the sample was allowed to warm up to room temperature and characterised once again by HAADF STEM. Fig. SI3 shows the reappearance of a uniform layer of liquid Hg around the NWs. The fact that the system is capable of reversing to its original appearance even after such strong temperature variation is an important result. Therefore it is assumed that the presence of mercury would not be a limiting factor for the life time of molecular electronics based on these technologies. *In situ* electrical measurements were performed at room temperature in order to confirm the maintained metallicity of the Hg//MoSI nanowire complexes. Fig. 6 shows a small bundle of Hg//MoSI nanowires in contact with the tungsten tip with the corresponding linear *IV* curve in Fig. 6b showing Ohmic behaviour with a bundle resistance of 264 kΩ.

3.3. Control over the assembly process

For assembly of nanomaterials, the energy control of mixing systems is important.[17,18] Because of their high surface energy, spontaneous bundling of nanowires is an energetically beneficial process, corresponding to a reduced global free energy.[4] The presence of sulphur and iodine located at the surface of nanowires favors their dispersion stability in organic solvents like acetone. However, such dispersability could have some selectivity to organic solvents due to the difference in solubility parameters. This implies that for a given system, control of the energy will be an important means to manipulate the assembly of nanowires by tuning interaction enthalpy or mixing entropy. In order to very this we tested two solvents having very different surface tensions, acetone (E_{sur} = 23.7 mJ m^{-2} at 20 °C) and water (E_{sur} = 72.8 mJ m^{-2} at 20 °C), proving to be equally suitable dispersants to promote the interaction between mercury and MoSI nanowires. Water did not seem to inhibit the nanowire assembling process. It was also interestng to note that under identical preparation conditions (same nanowire concentration = 0.1 mg ml^{-1}; Hg/MoSI ratio of 1 to 10; 1 month aging time) the water based dispersion gave rise to networks of nanowire bundles of much bigger diameter than the ones obtained in acetone, as shown in the TEM image in Fig. 7. This image can be directly compared to the ones obtained for acetone based dispersions (Fig. 2a, 3, 4 and 5), immediately noticing that the

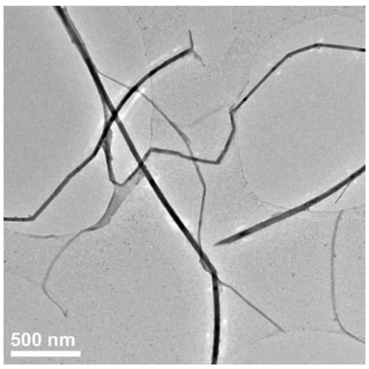

Fig. 7 TEM image of a Hg//MoSI nanowire network produced in water.

nanowire bundles in water are from 5 to 10 times bigger in diameter.

Therefore, the nature of the dispersant media seems to affect the aggregate structure but not the network formation. This observation is especially significant as it provides greater freedom in applications where the flexibility of working with different dispersant media or with nanowires bundles of different diameter can be differently chosen and controlled. A detailed study is currently in progress to determine whether other parameters, such as nanowire concentration, nanowire/mercury ratio or different sonication/stirring methods could be used to gain further control over the typology of architectures obtained (*i.e.* crosses *vs.* Y-type junctions).

Finally, in order to confirm the ultimate role of mercury during the assembly process and rule out the spontaneous organisation of nanowires in networks with time, an AFM control experiment was carried out on a dispersion of MoSI nanowires in absence of functionalising mercury. Fig. 8 shows typical AFM images for unfunctionalised $Mo_6S_3I_6$ nanowires dispersed in acetone at a concentration of 0.1 mg ml^{-1} immediately (a) and after four weeks (b) from preparation.

Herewith we demonstrate that aged unfunctionalised dispersions do not lead to self-assembled nanowire networks. The diameters of a large quantity of bundles were measured

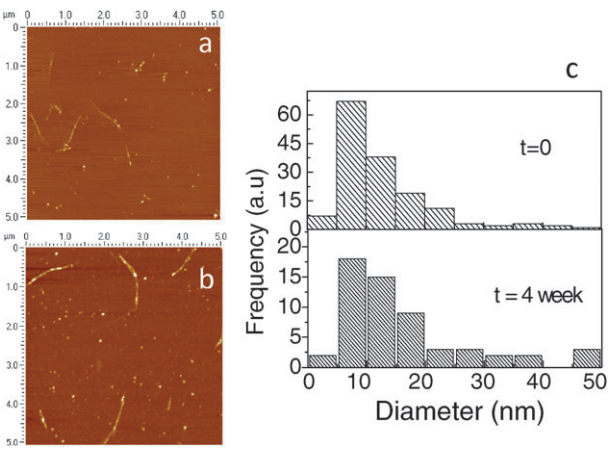

Fig. 8 AFM images for unfunctionalised $Mo_6S_3I_6$ nanowires dispersed in acetone immediately (a) and after four weeks (b) from preparation. The diameters of a large quantity of bundles were measured in both cases, leading to the diameters distributions in (c).

for a solution of unfunctionalised wires in acetone, immediately after preparation and after one month. These diameters were plotted as distributions in Fig. 8c. Statistical analysis shows that these distributions are indistinguishable within a 95.99% confidence interval. This clearly means that not only no network assembly has occurred but that the bundles have not re-aggregated considerably over the time scale of four weeks. This suggests that the dispersion is at least quasi-stable and may in fact be at or near equilibrium.

Ultimately, the choice of mercury as MoSI functionalising agent allows us to control the nanowire deposition on specific substrates and in the online supplementary information we show our first, very promising results over this attempt. In order to demonstrate this, we used focused ion beam (FIB) induced deposition to fabricate a pre-patterned substrate with the simple scope of proving the tailored interfacing properties of the Hg//MoSI complexes. With this aim in mind, a dielectric layer of silicon oxide (SiO_2) was deposited using the FIB onto a silicon substrate with 5 μm wide tungsten pads further deposited on top, at a distance of 2 μm from each other (Fig. SI4a). These distances were initially chosen to facilitate the positioning of Hg//MoSI nanowire bundles across the pads, taking into account an average nanowire length of 3 to 6 μm.[7] Tungsten was the chosen material for the pads being conductive and chemically affine to mercury. A drop of a solution of unfunctionalised nanowires was casted on the pads. The unfunctionalised nanowires showed no affinity for the substrate whatsoever. Fig. SI4b shows the SEM image of the only two nanowire bundles we found on the substrate in this case. The rest of the material was found to be re-aggregated at the borders of the silicon substrate. A completely different behaviour was instead observed when a drop f Hg//MoSI complex was casted onto the pre-patterned surface. Fig. SI4c shows a SEM image of the as deposited substrate demonstrating how the Hg//MoSI nanowire networks deposit and interface merely on the tungsten covered areas, leaving the surface between the tungsten pads relatively clean and wire-free. Only very few short aspect ratio nanowire bundles (<2 μm in length) can be seen on the silicon dioxide substrate, with the longer ones forming networks bridging and interconnecting two tungsten pads (Fig. SI4d).

Conclusions

In conclusion we have presented an innovative route for the production of self-assembled MoSI nanowire networks to be exploited for large functional nanocircuits. This method exploits the nominal high affinity that sulphur and iodine atoms have towards mercury. Full and uniform decoration of the nanowires with Hg has been obtained in solution using a common organic mercury salt as a source of single Hg atoms. We have used atomic force microscopy (AFM) to demonstrate the efficient formation of extended Hg-nanowire networks, whilst aberration corrected scanning transmission electron microscopy (STEM) and high-resolution transmission electron microscopy (HRTEM) have been used to show the nature and the evolution of the Hg//MoSI nanowire complexes over time. The degree of mercury coverage on the wires appears to be strongly time dependent, with average network formation time

of two weeks in solution. These results provide strong evidence for the formation of a liquid mercury coating both on the walls and the ends of the nanowires, ultimately leading to self-assembly of the nanowires into structured networks. *In situ* variable temperature (S)TEM experiments have shown crystallisation of the mercury coating upon cooling. *In situ* STM/TEM characterisation proves the maintained high conductivity and stability of the Hg//MoSI complexes, whilst the presence of mercury provides the means to tune and interface the nanowire networks at specific positions. This approach to facile functionalisation of MoSI nanowires in solution and the formation of adequate conductive networks represents a major accomplishment, raising the possibility of reproducibly self-assemble large complex circuits based on single molecules. Furthermore, the use of a functionalising agent as affine to many molecular species as mercury constitutes a main advantage to facilitate recognition, to allow interaction of the nanowires with other molecular species and to connect the nanowires to the outside world. This will make these systems exploitable in the efficient production of a variety of devices including nanosensors, nanoelectrodes and molecular switches.

This work was supported by: the Marie Curie IEF grant PIEF-GA 2008-220150 (VN), the Royal Academy of Engineering/EPSRC (VN). the Royal Society (NG), the STREP project BNC Tubes, NMP4-CT-2006-03350 (NG, ZA) and the ERC Starting Grant (ERC-2009-StG-240500) (NG, ZA). All authors thank BegbrokeNano for their provision of research facilities.

References

1 R. Sordan, K. Balasubramanian, M. Burghard and K. Kern, *Appl. Phys. Lett*., 2006, **88**, 053119.
2 G. K. Mor, O. K. Varghese, M. Paulose and C. A. Grimes, *Sens. Lett*., 2003, **1**, 42.
3 R. Saito, *Physical Properties of Carbon Nanotubes*, Imperial College Press.
4 S. Bergin, V. Nicolosi, P. Streich, S. Giordani, Z. Sun, A. H. Windle, P. Ryan, P. P. Niraj, W. T. Wang, W. J. Blau, J. J. Boland, J. P. Hamilton and J. N. Coleman, *Adv. Mater*., 2008, **20**(10), 1876–1881.
5 D. Vrbanic, M. Remškar, A. Jesih, A. Mrzel, P. Umek, P. Ponikvar, B. Jančar, A. Meden, B. Novosel, S. Pejovnik, P. Venturini, J. C. Coleman and D. Mihailović, *Nanotechnology*, 2004, **15**, 635.
6 V. Nicolosi, D. Vrbanic, A. Mrzel, J. McCauley, S. O'Flaherty, D. Mihailovic, W. J. Blau and J. N. Coleman, *Chem. Phys. Lett*., 2005, **401**, 13.
7 V. Nicolosi, D. Vrbanic, A. Mrzel, J. McCauley, S. O'Flaherty, C. McGuinness, G. Compagnini, D. Mihailovic, W. J. Blau and J. N. Coleman, *J. Phys. Chem. B*, 2005, **109**, 7124–7133.
8 D. McCarthy, V. Nicolosi, D. Vengust, D. Mihailovic, G. Compagnini, W. J. Blau and J. N. Coleman, *J. Appl. Phys*., 2007, **101**, 014317.
9 V. Nicolosi, D. Vengust, D. Mihailovic, W. J. Blau and J. N. Coleman, *Chem. Phys. Lett*., 2006, **425**, 89–93.
10 V. Nicolosi, D. McCarthy, D. Vengust, D. Mihailovic, W. J. Blau and J. N. Coleman, *Eur. Phys. J.: Appl. Phys*., 2007, **37**, 149.
11 M. Uplaznik, B. Bercic, J. Strle, M. I. Ploscaru, D. Dvorsek, P. Kušar, M. Devetak, D. Vengust, B. Podobnik and D. Mihailovic, *Nanotechnology*, 2006, **17**, 5142.
12 I. Vilfan and D. Mihailovic, *Phys. Rev. B: Condens. Matter Mater. Phys*., 2006, **74**, 235411.
13 V. Nicolosi, P. D. Nellist, S. Sanvito, E. C. Cosgriff, S. Krishnamurthy, W. J. Blau, L. M. H. Green, D. Vengust, D. Dvorsek, D. Mihailovic, G. Compagnini, J. Sloan, V. Stolojan, J. D. Carey, S. J. Pennycook and J. N. Coleman, *Adv. Mater*., 2007, **19**(4), 543–547.
14 M. I. Ploscaru, S. J. Kokalj, M. Uplaznik, D. Vengust, D. Turk, A. Mrzel and D. Mihailovic, *Nano Lett*., 2007, **7**(6), 1445.
15 P. D. Nellist, M. F. Chisholm, N. Dellby, O. L. Krivanek, M. F. Murfitt, Z. S. Szilagyi, A. R. Lupini, A. Borisevich, W. H. Sides and S. J. Pennycook, *Science*, 2004, **305**, 1741.
16 P. D. Nellist and S. J. Pennycook, *Advances in Imaging and Electron Physics*, 2000, **113**, 148.
17 Y. J. Min, M. Akbulut, K. Kristiansen, Y. Golan and J. Israelachvili, *Nat. Mater*., 2008, **7**, 527–538.
18 K. J. M. Bishop, C. E. Wilmer, S. Soh and B. A. Grzybowski, *Small*, 2009, **5**(14), 1600–1630.

